

# Background Document

## FEMA P-58/BD-3.9.8

# Fragility of Masonry Parapets

Prepared by

John Oстераas, Exponent, Menlo Park, California  
Helmut Krawinkler, Stanford University, Stanford, California

Submitted to

APPLIED TECHNOLOGY COUNCIL  
201 Redwood Shores Parkway, Suite 240  
Redwood City, California 94065  
[www.ATCouncil.org](http://www.ATCouncil.org)

Prepared for

FEDERAL EMERGENCY MANAGEMENT AGENCY  
U.S. Department of Homeland Security  
500 C Street, SW  
Washington, D.C. 20472

December 28, 2010



**FEMA**



## **Background Documentation**

---

FEMA P-58 Background Documents are a series of reports documenting the technical background and source information for key aspects of the FEMA P-58 methodology and its implementation. These reports were developed over the course of the 10-year ATC-58/ATC-58-1 Projects funded under FEMA Contracts EMW-2001-RP-0056 and HSFEHQ-06-D-1105.

Background Documents were developed by consultants, serving at various levels within the project hierarchy, reporting the results of: (1) decisions on technical development protocols; (2) focused studies on the development of key aspects of the methodology; (3) documentation of recommended procedures; and (4) collection of available data for the development of structural and nonstructural fragilities. They were initially intended to serve as a record of the technical state-of-knowledge at the time they were produced, and as resources for the development of the eventual project reports. As such, they represent a snapshot in time, and may, or may not, match the technical content, recommended procedures, or data incorporated into the final methodology and its implementation.

This Background Document is intended for the purpose of providing supplemental knowledge to users of the FEMA P-58 methodology. Information contained herein has not been independently verified for accuracy as a stand-alone document, and may have been superseded in its final implementation within the methodology. Specifically in the case of certain nonstructural component fragilities, the NISTIR fragility classification numbering scheme was modified over the course of the project, and the fragility classification number assigned in this document might be different from numbers assigned in the final fragility database. Users of information in this document assume all liability arising from such use.

## **Notice**

---



Any opinions, findings, conclusions, or recommendations expressed in this publication do not necessarily reflect the views of the Applied Technology Council (ATC), the Department of Homeland Security (DHS), or the Federal Emergency Management Agency (FEMA). Additionally, neither ATC, DHS, FEMA, nor any of their employees, makes any warranty, expressed or implied, nor assumes any legal liability or responsibility for the accuracy, completeness, or usefulness of any information, product, or process included in this publication. Users of information from this publication assume all liability arising from such use.

Cover illustration – Primary resource documents for the FEMA P-58 *Seismic Performance Assessment of Buildings, Methodology and Implementation* series of products: FEMA P-58-1, *Volume 1 – Methodology*, and FEMA P-58-2, *Volume 2 – Implementation Guide*.

# Fragility of Masonry Parapets

John Osteraas and Helmut Krawinkler (12/28/2010)

**Table 1. Summary results**

Fragility, damage measures, and consequences for:		
Component category:	Masonry Parapets	
Basic composition:	Unreinforced and unbraced masonry parapets as a component of masonry buildings. Aspect ratio limits (parapet height-to-width ratio) of approximately three.	
Units:	Single parapet (along each face of building) at mid-span of parapet	
Demand parameter:	Peak horizontal ground acceleration (PGA); spectral acceleration at T=1 sec. (Sa(1 sec.)); spectral acceleration at T=0.35 sec. (Sa(0.35 sec.)); peak roof velocity (PRV) at T=0.35 sec.	
Number of damage states:	2	
Damage states are:	<input checked="" type="checkbox"/> ordered; <input type="checkbox"/> mutually exclusive; <input type="checkbox"/> simultaneous	
Authors and date:	B McDonald, J Hunt; H Krawinkler, J Osteraas, December 2010	
Damage states, fragilities, and consequences		
	DS1	DS2
Description:	Cracking with offset > 1/16"	Toppling of all or portion
Illustration:		
Median demand (θ):	0.2g PGA 0.2g Sa(1 sec.) 0.4g Sa(0.35 sec.) 13 in/sec PRV	0.4g PGA 0.4 g Sa(1 sec.) 0.8g Sa(0.35 sec.) 27 in/sec PRV
Dispersion (β) <sup>(1)</sup> :	0.6 for each demand parameter	0.6 for each demand parameter
Probability <sup>(1)</sup> :		
Correlation:		
Repairs required:	Replace and reinforce	Replace and reinforce
Possible consequences:		
Repair cost (Y/N/?):	Y	Y
Death, injury (Y/N/?):	N	Y
Inoperative (Y/N/?):	N	Y
Red tagging (Y/N/?)	N, “Yellow Tag” marked with area unsafe	Y – Likely “Red Tag” or possibly “Yellow tag” marked with area unsafe

**Table 2. Supporting information summary**

## **Introduction**

It is axiomatic that masonry parapets are one of the most fragile building components. Virtually all post-earthquake reconnaissance reports mention the number of damaged or toppled parapets observed. While these data reinforce the fragile nature of masonry parapets, like most field data reviewed, there is no data on the number of parapets that were undamaged. A number of studies based on much smaller data sets do report the number of damaged as well as undamaged parapets, though the data sets are quite small, especially for higher intensities of ground shaking. Thus, little of the available data are useful for developing fragility functions.

Unlike other building components which are generally standardized, construction of parapets is typically based on architectural requirements as opposed to standard designs, engineered or not. Prescriptive design features have made their way into building codes over the decades, but even these (e.g., nominal steel reinforcement, anchorage to diaphragms) are often not explicitly designed, employ questionable construction detailing and are of highly variable construction quality. Not surprisingly, implementation of these prescriptive requirements has resulted in mixed improvement of parapet seismic performance. Areas of similar construction can exhibit not only a wide range of damage severity, but also a large number of damage modes. As a consequence, the response of this seemingly simple component is in reality quite complicated: First, one cannot rely on the strength or ductility of key components such as mortar, wall or roof ties, reinforcing bond/development, etc. Second, the onset of substantial nonlinearity associated with first cracking and onset of rocking or sliding of all or part of the parapet can occur at low intensity and early in the ground shaking record. For instance, the restoring moment of a cracked, free-standing parapet acting as a rocking rigid block decreases as block rotation increases. In addition, incorporation of stiffness and strength degradation due to rocking, mortar crushing, damage to adjacent components, etc., is difficult, at best, to model realistically.

## **Demand Parameter**

PGA was selected as the primary demand parameter, because empirical data were available for this parameter. Other demand parameters including PGV, PGD, PGV/PGA Spectral Acceleration, Effective PGA, Story Drift, and Peak Roof Acceleration were considered. Peak roof velocity (PRV) at  $T=0.35$  sec., spectral acceleration at  $T = 1$  sec. ( $Sa(1 \text{ sec.})$ ), and spectral acceleration at  $T = 0.35$  sec. ( $Sa(0.35 \text{ sec.})$ ) were also selected to generate fragility curves for comparison.

## **Damage States**

Numerous parapet damage states are observed following earthquakes, ranging from complete collapse to damage that can only be identified by careful inspection of the parapet. Available data sets contain little information on the nature of the parapet damage observed. After considerable effort to develop fragility functions for various parapet configurations for multiple damage states using either empirical data or analytical studies, it was concluded that neither approach would provide defensible fragility functions. Rather, a hybrid approach based on professional judgment informed by the insight gained from analysis of empirical data and numerical simulation of parapet response was adopted to develop fragility functions for two damage states (cracking with visible offset and toppling of a portion of the parapet). DS1 captures those conditions where damage would be readily apparent (i.e. visible cracking, leaning of the

parapet away from the building), likely resulting in a Yellow Tag – Area Unsafe, and requiring removal or replacement. DS1 does not include damage that can only be identified with a detailed inspection of the parapet. Thus, subtle damage is not reflected in the statistics for DS1. DS2 captures all toppling damage that has potential for human injury or death.

## Empirical Data

Damage to parapet walls in unreinforced masonry buildings from the 1989 Loma Prieta and 1994 Northridge earthquakes are described in field reports by Lizundia *et al.* (1991, 1997a, 1997b). Data files that accompanied the Lizundia reports indicated damage or no damage (Yes/No) to parapets. Comment fields in the survey forms listed some different types of damage (cracking, falling hazard, etc.); however, in most cases detailed descriptions of damage was limited. Seismic intensity measures (PGA, PGV, MMI, etc.) for the observed locations were obtained from ShakeMaps. The number of surveyed unreinforced masonry buildings in the Loma Prieta survey was 463, and the number of surveyed unreinforced masonry buildings in the Northridge survey was 93. A summary of the observed cases of sliding (DS1) and toppling damage (DS2) is shown in Figure 1. The median and dispersion values that fit a logarithmic cumulative distribution through these points are approximately 0.4g and 0.6, respectively. The median and dispersion values were determined using the maximum likelihood curve fitting algorithm provided by Baker and Zarein (2009).

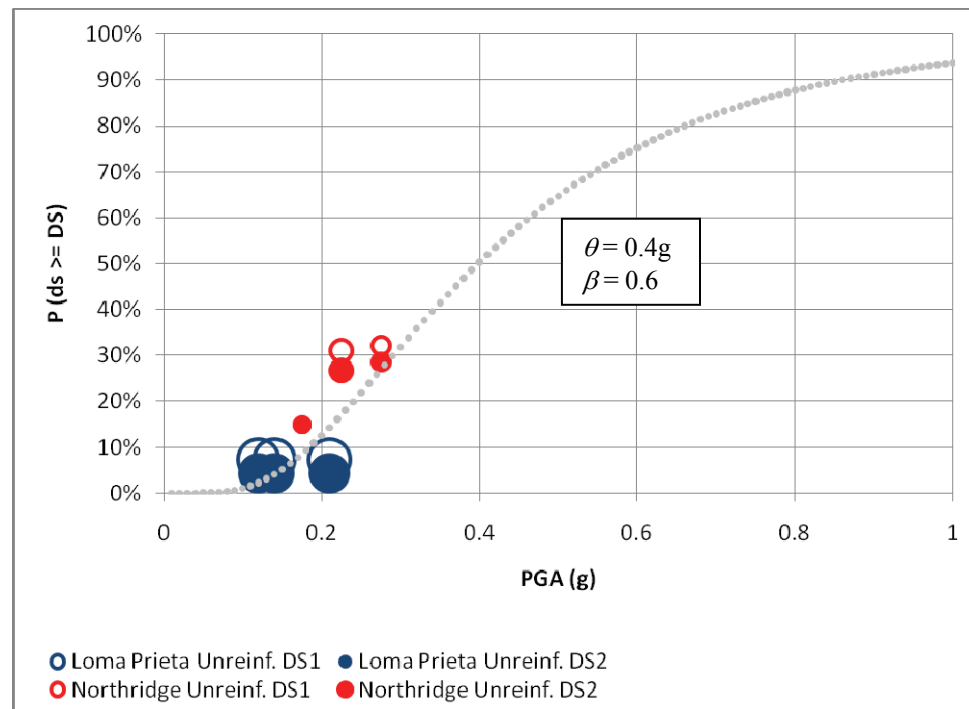


**Figure 1.** Fragility data for observed unreinforced parapet damage in Loma Prieta and Northridge earthquakes

## Data from Analytical Studies

**Review of past analytical studies.** A basic assumption in this review is that parapets are simple cantilever elements with negligible bending strength at the roof line and with negligible restraint provided by plate action, i.e., parapets can be treated as rigid blocks that will slide and ultimately

overturn as the intensity of the ground motion increases. Many analytical studies have been performed in the past 50 years on rocking and overturning of rigid blocks. Most studies do not address explicitly the combination of rocking plus sliding, but much of the past work may be applicable to the response of masonry parapets after initial cracking at the base.

An early and important study of the rocking of rigid blocks by Housner (1963) explored anomalous damage observations after several earthquakes, namely, the survival of tall slender monuments and structures in areas where their squat and apparently stable counterparts were severely damaged. Housner investigated rocking of rectangular blocks on rigid bases undergoing constant, sinusoidal and earthquake ground motions. His key results included analytic expressions for the effective period of rocking, which tends to infinity as the rocking angle approaches the point of imminent overturning. Housner also showed that there is a size effect, that is, the propensity for overturning is not governed solely by aspect ratio, and that dynamic survival is not predicted by simple statics.

Since Housner's paper there have been many researchers who have advanced this topic: we identify a few here, but acknowledge this is by no means an exhaustive list. Alsam et al (1980) carried out a series of shake table tests of rigid block rocking and showed that the response is very different from classical structural systems. In fact, the block was so sensitive to input parameters that experimental results using earthquake ground motions were not repeatable, much less predictable. Ishiyama (1982 and 1984) developed a computer program to simulate the response of a rigid block that included rocking, sliding, and jumping, alone and in combination. Through analysis and testing, he showed that any criterion for overturning needed to include both peak acceleration and peak velocity, and provide expressions for predicting overturning failures. Yim, Chopra and Penzien (1980) also showed through numerical simulation that the response of a rigid block is very sensitive to block size, aspect ratio and characteristics of the ground motions. While individual responses could differ, they showed that in a probabilistic sense the vulnerability to overturning increases with aspect ratio and motion intensity, and decreases with block size. Their paper provides plots showing cumulative probability distributions for overturning as a function of ground motion intensity measures, based on numerical simulation using synthetic ground motions. Spanos and Koh (1984) defined the governing differential equations for rocking blocks and used numerical integration to show, among other things, combinations of frequency and amplitude that lead to overturning for differing block aspect ratios. More recently, Sharif et al (2007) and Meisl et al (2007) have investigated probabilistic failure criteria for rocking of block walls with anchorage to diaphragms.

Purvanche et al. (2008) used Monte Carlo simulations and logistic regression analysis to quantify overturning fragilities of a rigid block subjected to earthquake-like random vibration waveforms. Their primary configuration variables are the aspect ratio  $B/H$  and the frequency parameter  $p = \sqrt{(mgR/I)}$ , and their primary demand variables are PGA and the ratio PGV/PGA. They also performed shaking table tests to calibrate their results. From the plots presented in their paper, it is estimated that the median overturning capacity, expressed in PGA, for the range of PGV/PGA ratios from about 0.05 to 0.20 varies from about 0.75g to 0.35g. The capacity clearly decreases with an increase in the PGV/PGA ratio, demonstrating the importance of velocity pulses. The implications of their conclusions for parapets is not clear because parapets are not subjected to ground motions; their response is driven by the motions of the roof of the structure on which the parapet rests.

In summary, past studies verify the large expected scatter in the response of block-like structures (such as parapets and chimneys) to earthquake-generated motions, and the lack of deterministic equations available for predicting toppling—much less any of the other potential parapet damage modes. None of these studies treated the structure as a filter that modifies the input motions, which are transmitted from the roof to the parapet, and not from the ground to the parapet.

From past work, and from mechanics principles, it becomes clear that toppling and sliding of parapets depends on geometric and material parameters and boundary conditions, as well as on the frequency characteristics of the motion to which the parapet is subjected. In the simplest idealized case, a parapet could be represented by a single rigid block subjected to rocking (defined by  $\theta$ ) and sliding (defined by  $\delta$ ) as illustrated in Figure 2.

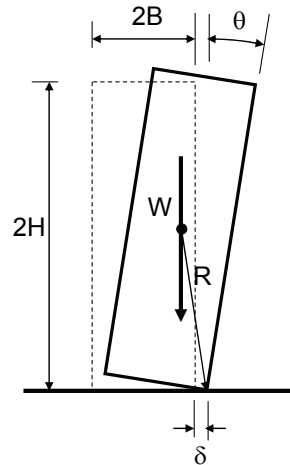


**Figure 2.** Rocking and sliding of rigid rectangular block

The response of this idealized rigid body depends on the following parameters (and others not itemized here):

- Dimensions B and H (aspect ratio  $H/B$ );
- Size and mass (or weight  $W$ );
- Frequency parameter  $p = \sqrt{(mgR/I)}$ ;
- Coefficient of restitution;
- Coefficients of static and dynamic friction;
- Peak acceleration of roof motion (PRA), relevant for uplift;
- Peak velocity of roof motion (PRV) and pulse characteristics of roof motion; and
- PRV/PRA ratio.

Using these parameters in analytical predictions of sliding and toppling, fragility curves for parapets do not consider variations in boundary conditions and material properties such as mortar crumbling that will reduce the effective width ( $2B$ ) of the rigid block. These variations will have to be accounted for by an increase in the dispersion. Moreover, variations in roof motion characteristics cannot be incorporated comprehensively in an analytical fragility curve prediction. To overcome this shortcoming, it was decided to use a single but comprehensive set of ground motions in order to account for record-to-record variability, and a single structure period ( $T = 0.35$  sec.) in order to account for the amplification of motion from the ground to the center of the diaphragm on which the parapet rests. A similar approach has been used in other ATC projects, such as ATC 63, i.e., FEMA P695, in which record-to-record variability is accounted for by using a relatively large set of representative ground motions, and modeling uncertainties are accounted for by inflation of the dispersion. This approach is employed in the Working Model 2-D study summarized below.

### **Results from Study with “Working Model 2-D”**

Considering the disparity of results obtained in various analytical studies on rocking of rigid blocks, and the apparent sensitivity of the results to roof motion frequency characteristics, the need was evident for comprehensive simulations of parapet failure modes using a set of representative ground motions as input to a structure whose roof motion serves as input to a rigid block representing the parapet and is of sufficient intensity to trigger the postulated failure modes of sliding and toppling. This study focused on the response evaluation of parapets using the dynamic simulation software Working Model 2-D. The software permits simulation of ground motion on a shaking table and representation of structures by means of rigid bodies and springs. Results from this program for wall rocking have been compared to experimental results of shaking table tests (Sharif et al., 2007) and have provided accurate predictions of seismic response.

The parapet is assumed to be free-standing and not structurally connected to the roof structure, appropriate assumptions for older vintage parapet walls or poorly constructed modern parapets that have suffered cracking at the base and full partial detachment from the structure early in the time history. The parapet was modeled as a rigid block resting on the edge of a simple elastic portal frame that represents the lateral response at mid-span of a diaphragm of a typical masonry building. The portal frame rests on a rigid table surface accelerated horizontally with a set of ground motions. The portal frame was modeled with inextensible elements with infinite rigidity in flexure joined with simple pinned connections, see Figure 3. The lateral stiffness and damping were modeled with an elastic spring and dashpot spanning the diagonal of the portal frame and were tuned to represent the expected behavior of common two-story commercial masonry buildings. At mid-span of the roof diaphragm, the drift comes from two main components: the global building lateral deflection (from the flexibility of the vertical lateral resisting system) and the diaphragm deflection (from the flexibility of the diaphragm), see Figure 4. The spring stiffness was calculated based on an assumed first mode period of 0.35 sec. The damping ratio was chosen as 0.05.

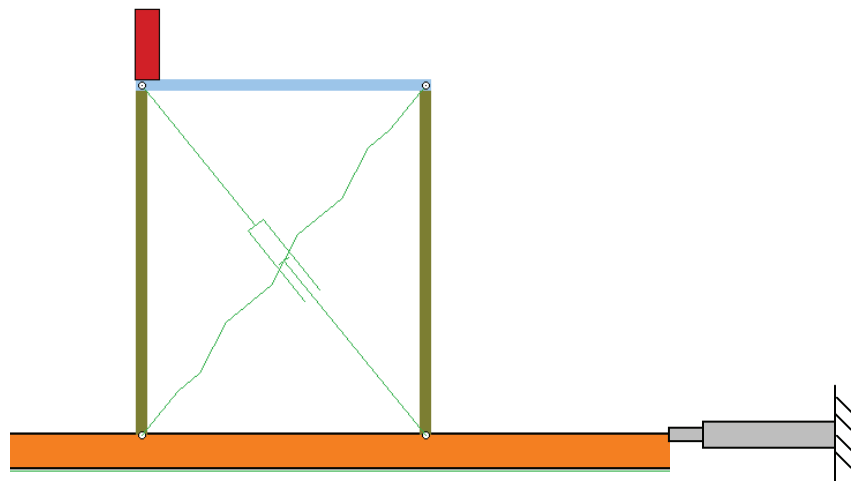


**Figure 3.** Working Model analytical model of free standing parapet on roof



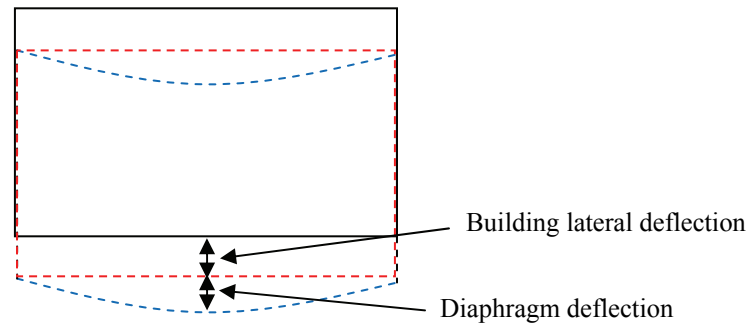
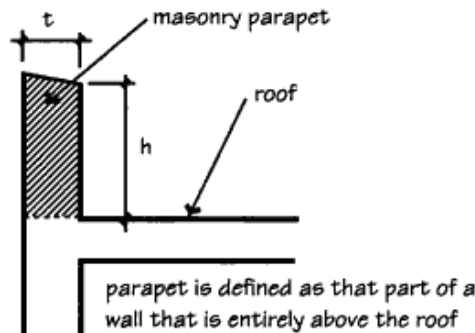


**Figure 4.** Plan view of roof diaphragm showing building and diaphragm deflections

The size of the parapet was based on the following considerations. The minimum thickness of parapet walls given in masonry design standards (i.e. Bealle 2003) is 8 inches (corresponding to a 2-wythe-thick parapet), and the maximum height to thickness ratio is 3. Thus, for a 2-wythe-thick (8 in.) parapet, the maximum height should be 24 inches, and for a 3-wythe-thick (12 in.) parapet, the maximum height should be 36 inches. In this study, the fragilities for a 36 in. by 12 in. parapet and 24 in. by 8 in. parapet are investigated. The design requirements for masonry parapets are summarized in Table 3.

**Table 3.** Masonry design standard parapet width and height limits (Bealle 2003)



Masonry Parapet Wall Requirements	
Requirement	MSJC*
Minimum thickness (t)	
solid masonry units	8 in.
hollow masonry units	8 in.
Maximum h/t ratio for unreinforced masonry parapets	
solid masonry units	3
hollow masonry units	3
Maximum height of unreinforced masonry parapets	
solid masonry units	3t
hollow masonry units	3t
Maximum wind loads for unreinforced parapets	110 mph basic wind speed
Steel reinforcement required	Seismic Design Categories D, E and F

\* Based on requirements of the Masonry Standards Joint Committee *Building Code Requirements for Masonry Structures*, ACI 530/ASCE 5/TMS 402.)

The following properties of the parapet were used:

- Height x width = 36x12" and 24x8"
- Unit weight = 120 lb/ft<sup>3</sup>
- Coefficient of restitution = 0.02
- Coefficient of static and dynamic friction = 0.8 and 0.7

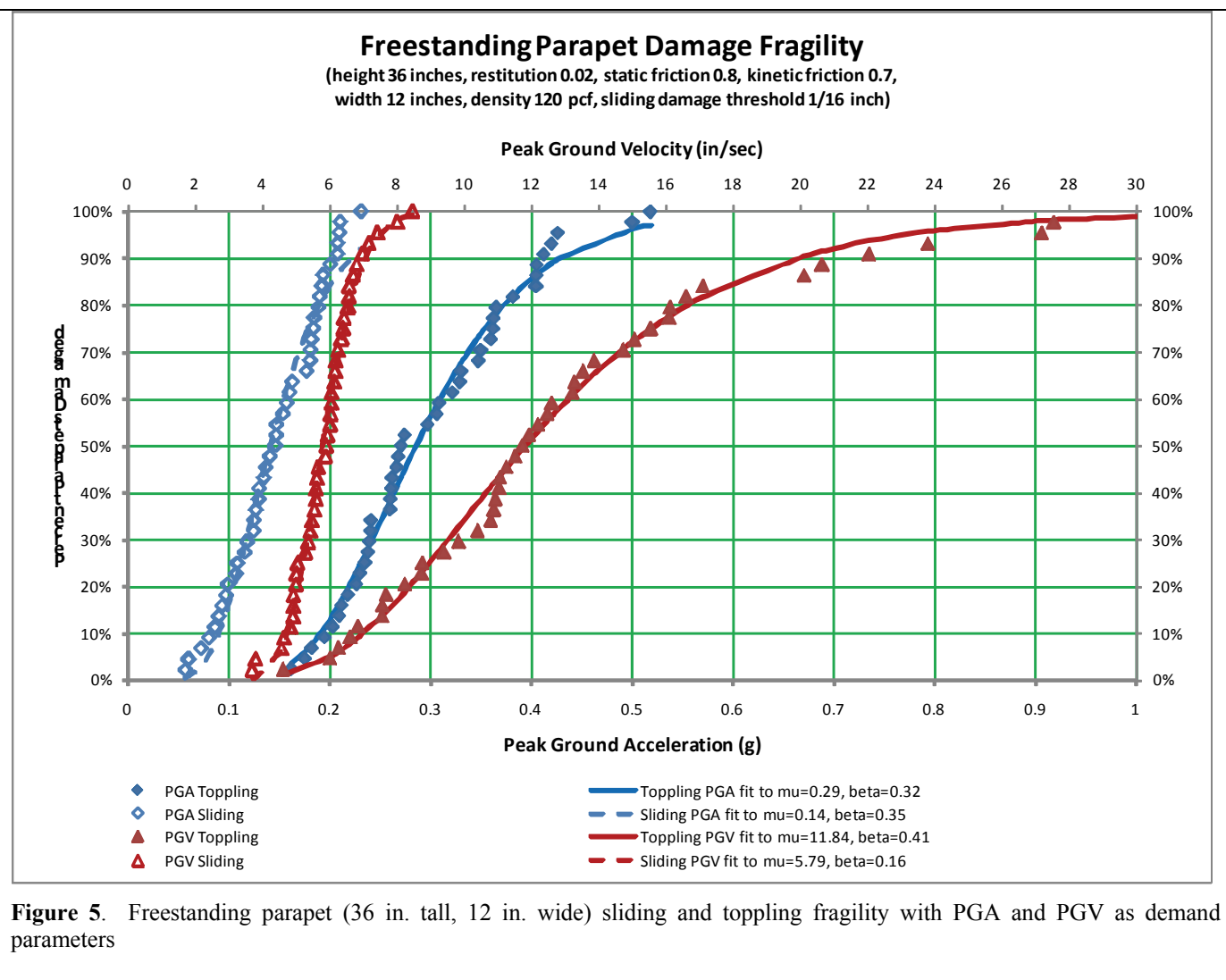
The coefficient of restitution appears to be small, but it provided the best match with experimental results reported in Sharif et al. (2007). Sensitivity studies did show that variations of the coefficient of restitution and friction coefficients had little effect on fragility curves.

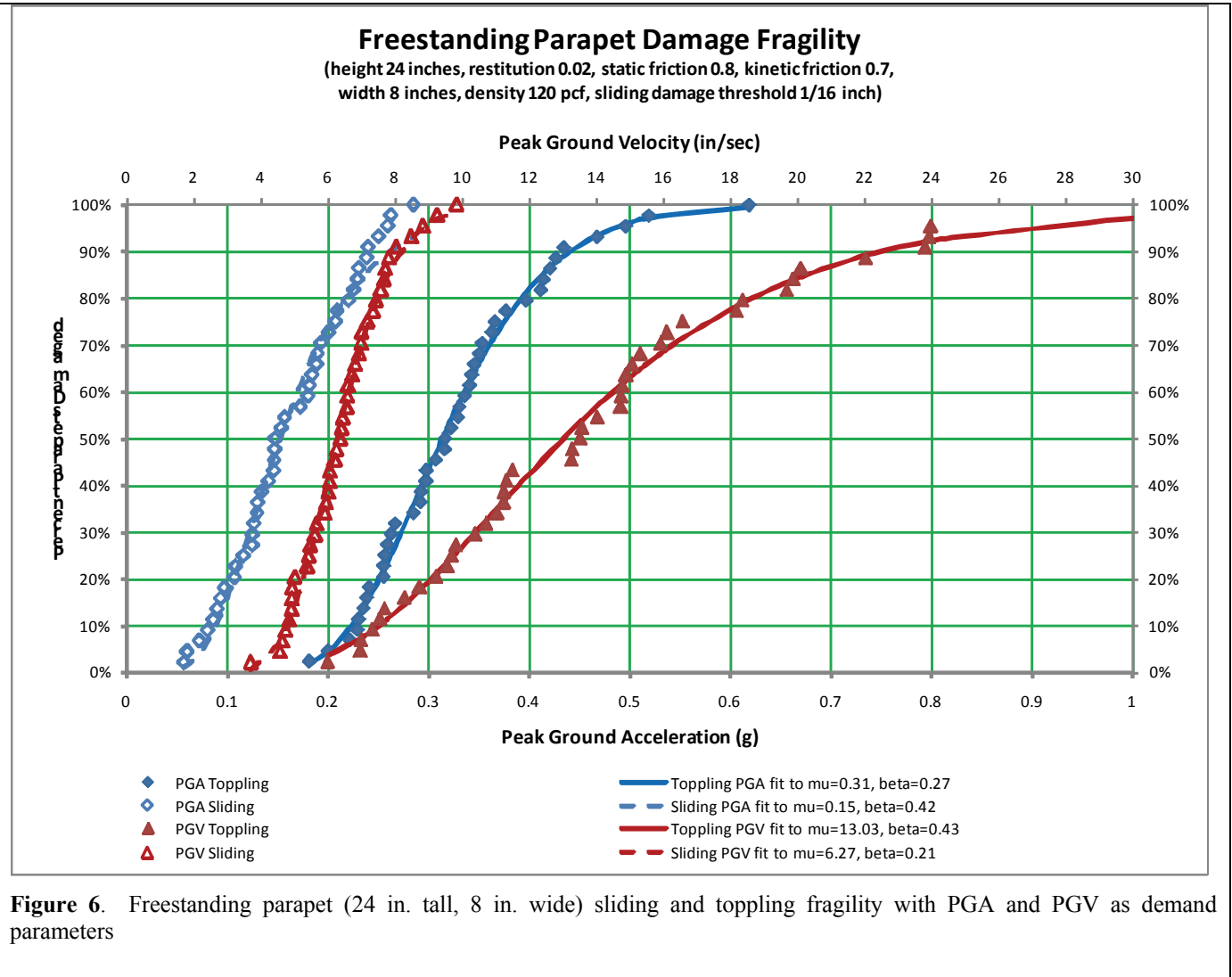
The structure with parapet was subjected to the FEMA P695 (ATC-63) set of 44 ground motion records (actually 22 pairs of records). This record set is discussed in detail in FEMA (2009). The records represent ground motions recorded at sites greater than 10km from the fault rupture. The records are intended to represent an unbiased suite of motions associated with earthquake magnitudes between 6.5 and 7.9.

Incremental dynamic analysis (IDA) was performed for each record, whereby the intensity of the record was increased until "significant" sliding and then toppling of the parapet occurred. The sliding capacity was defined as that ground motion intensity that causes sliding between the parapet and the roof diaphragm of at least 1/16". Toppling was defined as overturning of the parapet block.

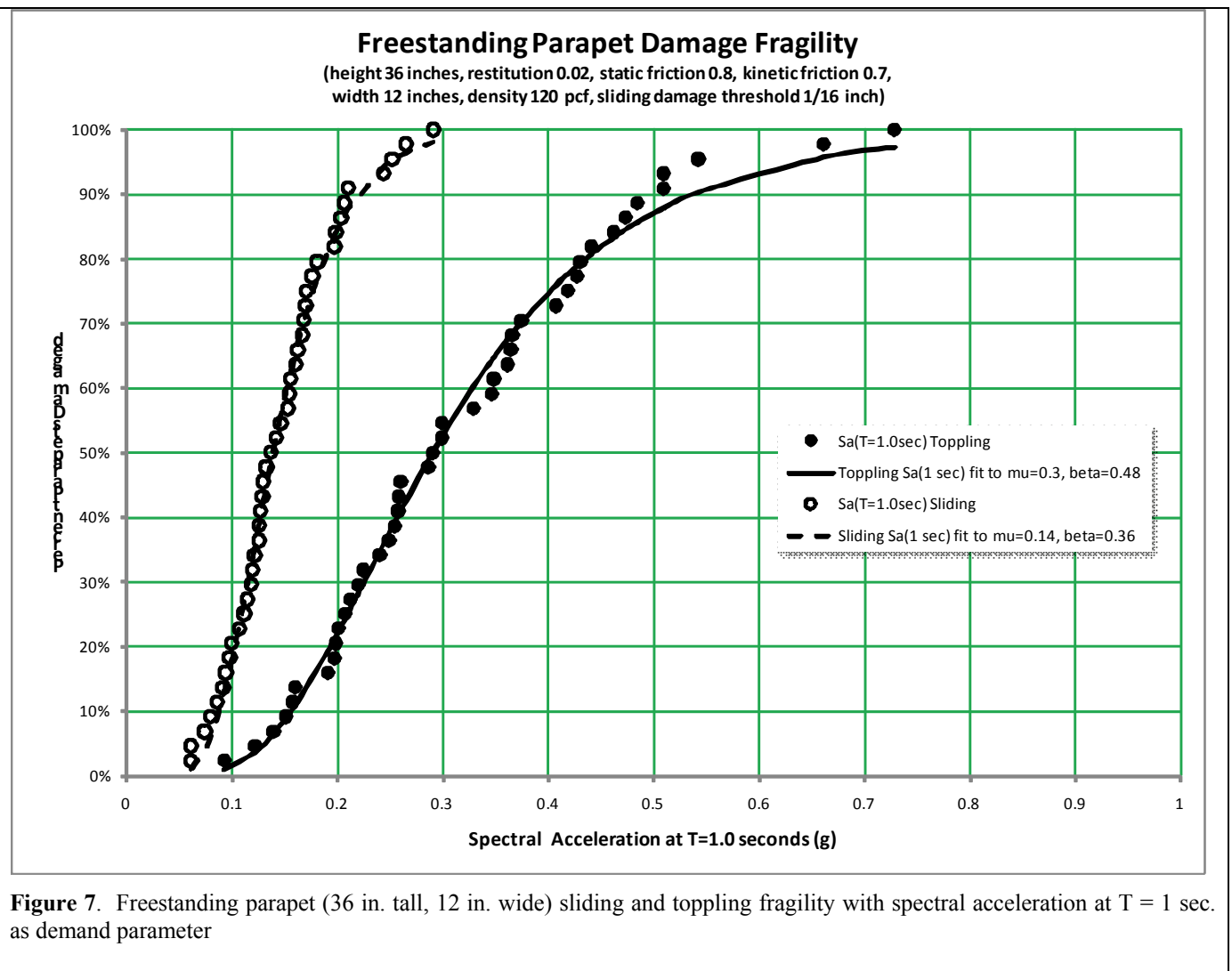
Various intensity measures (IMs) associated with the two failure modes were recorded, among them peak ground acceleration (PGA), peak ground velocity (PGV), spectral acceleration at  $T = 1$  sec. ( $S_a(1.0)$ ), spectral acceleration at  $T = 0.35$  sec. ( $S_a(0.35)$ ), and peak roof velocity (PRV) at  $T=0.35$  sec. The analysis results were post-processed by sorting each record by the IM value at the point of failure (sliding greater than 1/16", or toppling). The sorted records were used to assemble the empirical cumulative distribution functions (probability of failure given IM), and lognormal distributions were fit to the CDFs using least squares.

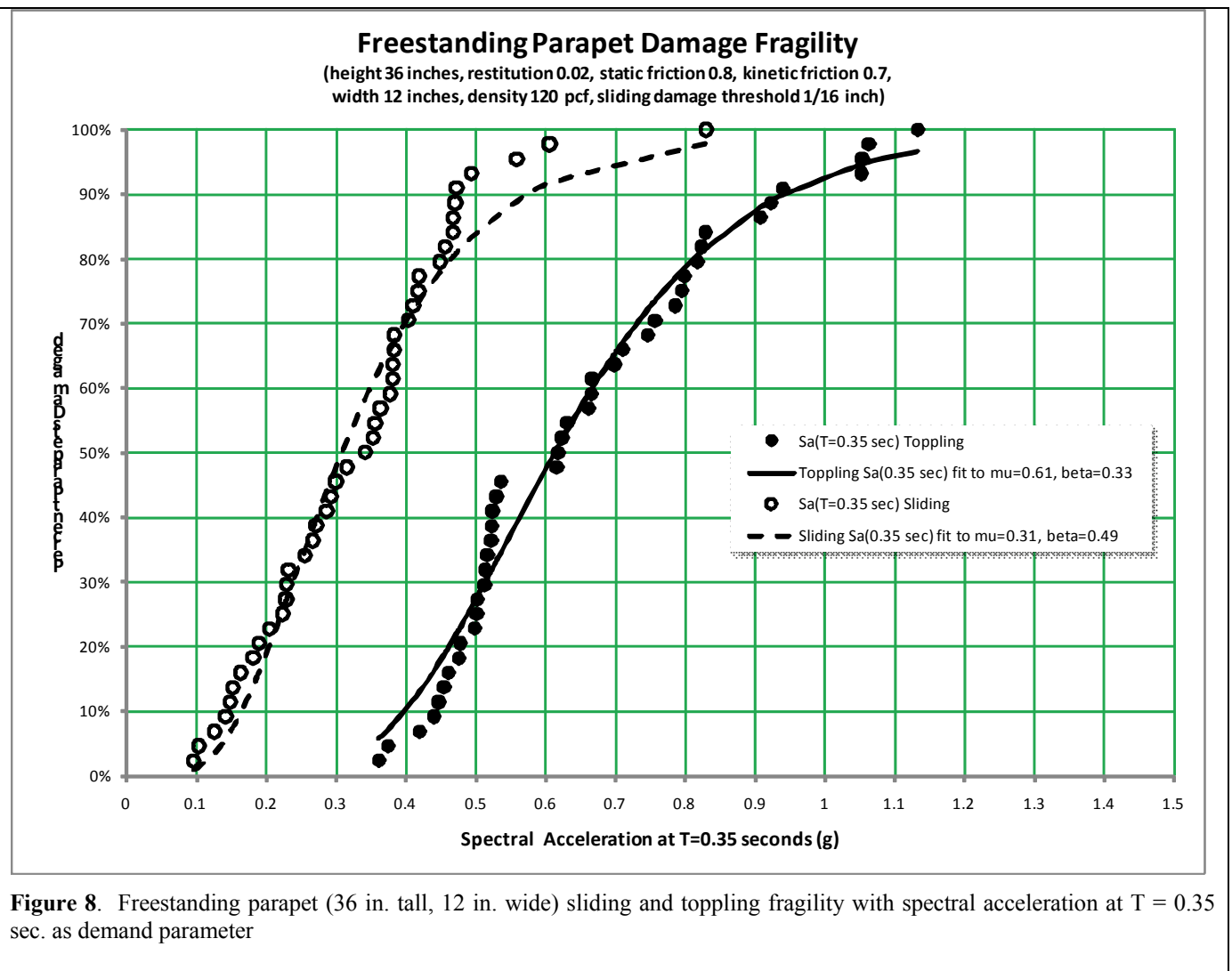
Figures 5 and 6 show sliding and toppling fragility curves for two parapet configurations (36x12" and 24x8"), using PGA (bottom scale) and PGV (top scale) as intensity measures. The differences between the 36x12" and 24x8" parapets are small, with an increase in capacity for the 24x8" case of about 10%. Median ( $\theta$ ) and logarithmic standard deviation values are shown in the figure legend. The dispersion ( $\beta$ ) is on the order of 0.3 to 0.4, i.e., relatively small, which is due to the unique structural filter ( $T = 0.35$  sec.) applied in all cases. There is no clear preference to the use of PGA or PGV as an intensity measure. Using PGA as the intensity measures provides a way to compare the fragilities with empirical data. Spectral acceleration at  $T = 1$  sec. ( $S_a(1 \text{ sec.})$ ),  $T = 0.35$  sec. ( $S_a(0.35 \text{ sec.})$ ), and peak roof velocity (PRV) at  $T = 0.35$  sec. were also used to generate fragility curves, as shown in Figures 7 - 9.





**Figure 6.** Freestanding parapet (24 in. tall, 8 in. wide) sliding and toppling fragility with PGA and PGV as demand parameters





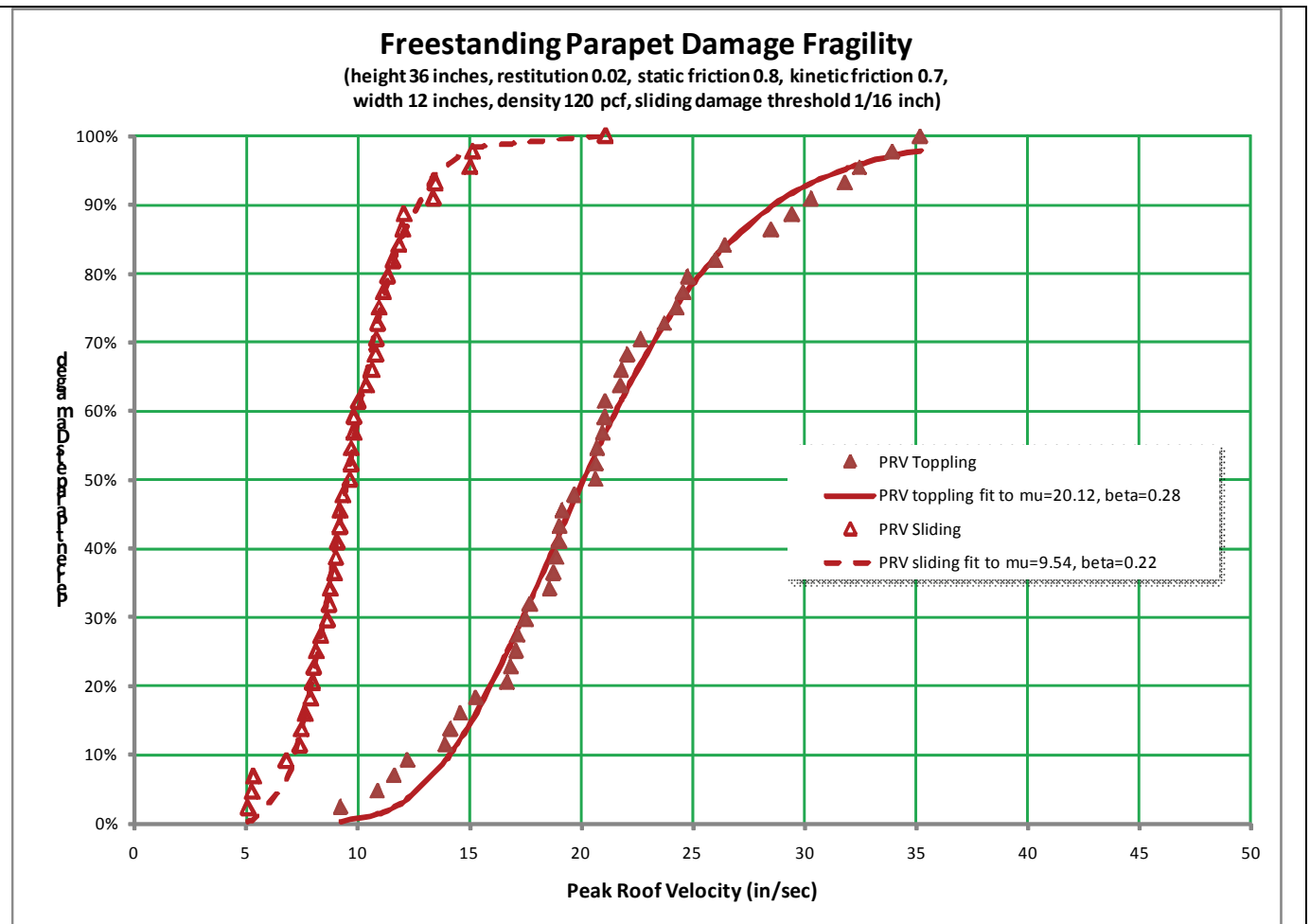


**Figure 9.** Freestanding parapet (36 in. tall, 12 in. wide) sliding and toppling fragility with peak roof velocity at  $T = 0.35$  sec. as demand parameter

The median value for sliding and toppling capacity is about 0.15g PGA and 0.30g PGA, respectively, i.e., very low. These values will depend strongly on the period of the structure/diaphragm system on which the parapet rests, and on the parapet aspect ratio. In this study  $T = 0.35$  sec. was used. At this period the spectral amplification of PGA for the selected ground motion set is about 2.3. For shorter and longer periods the amplification will be smaller, see Figure 10. Also, for smaller parapet aspect ratios the median capacities are expected to increase. Moreover, no credit is given in this analysis to restraining effect provided by plate action of the parapet. For these reasons an increase in median capacities appears to be justified. The following values are recommended: Median sliding capacity = 0.20g PGA, 0.20g Sa(1 sec.), 0.40g Sa(0.35 sec.), and 13 in/sec PRV, and median toppling capacity = 0.40g PGA, 0.40g Sa(1 sec.), 0.80g Sa(0.35 sec.), and 27 in/sec PRV. Considering the wide range of parapet aspect ratios and boundary conditions, and particularly the large uncertainty in the period of the structure/diaphragm on which the parapet rests, it is appropriate to use a large dispersion. A value of  $\beta = 0.6$  is recommended for both sliding and toppling. The recommended fragility curves for the sliding and toppling damage states are shown in Figure 11-14.

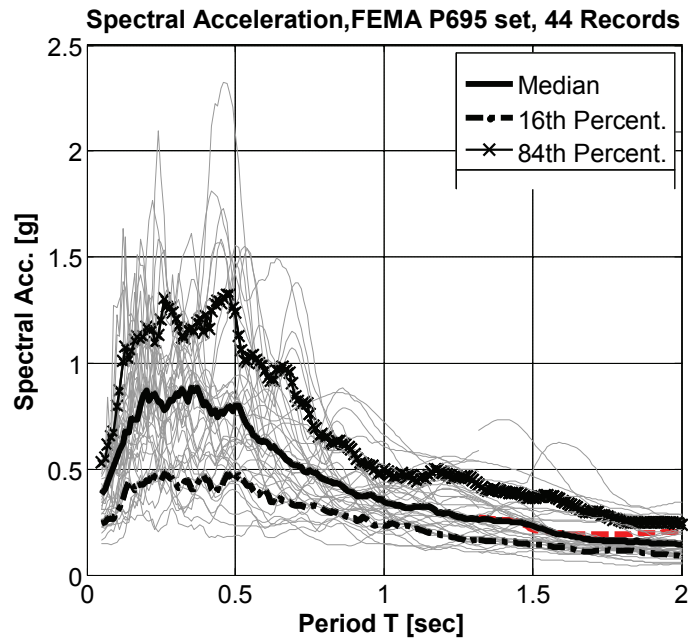


Figure 10. Spectra of normalized FEMA P695 ground motion set

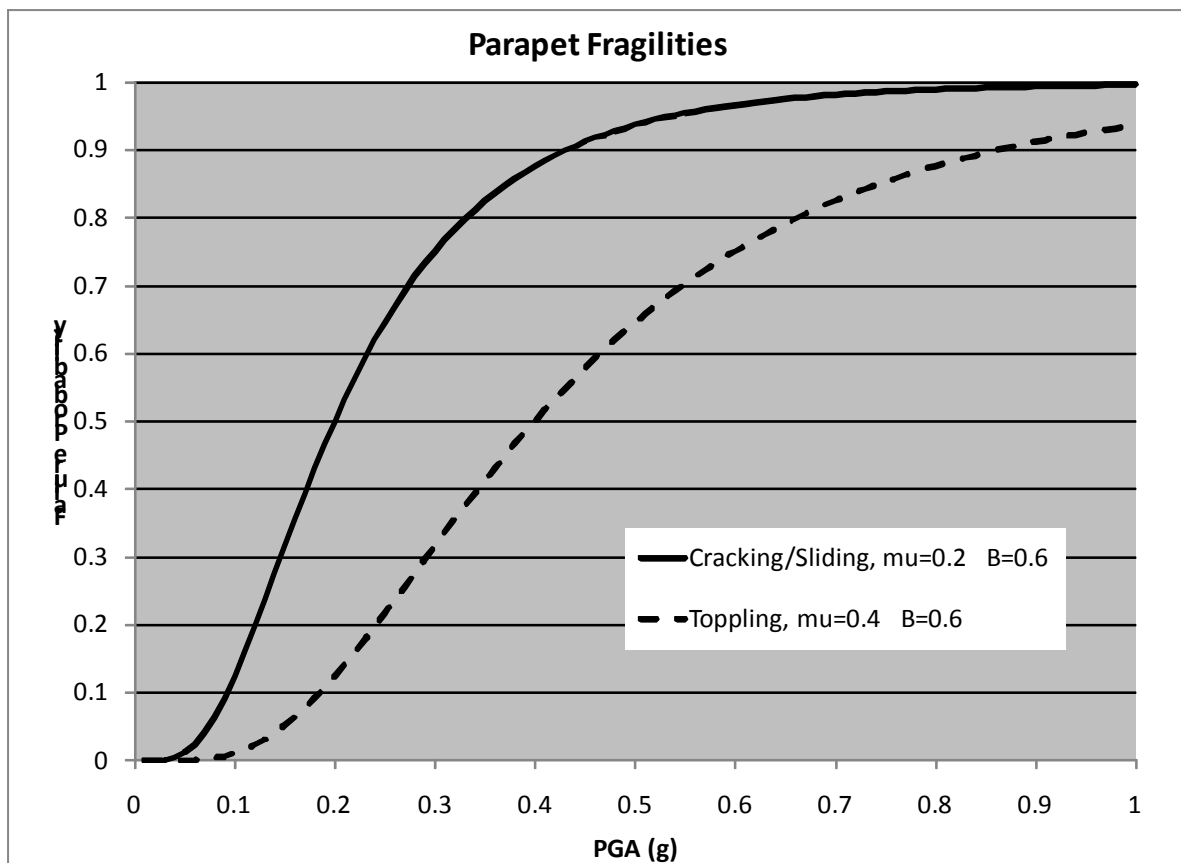
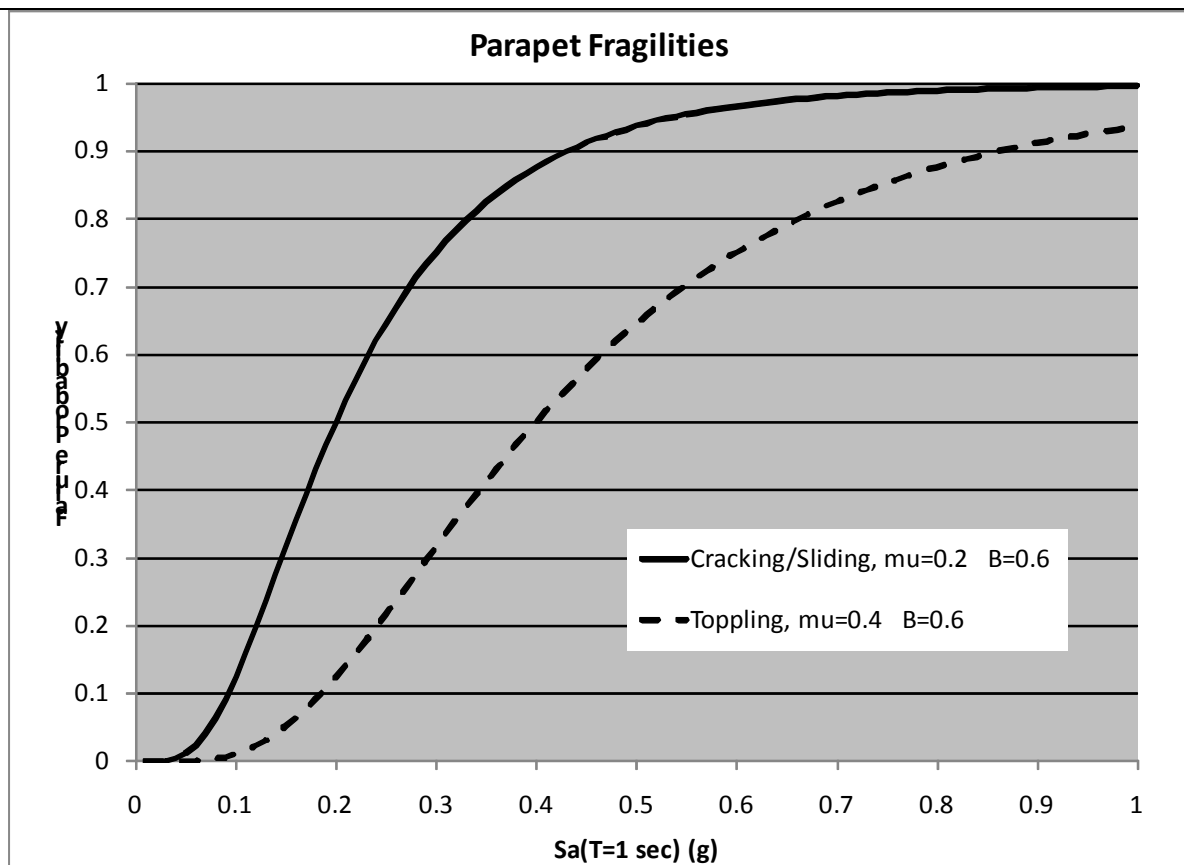
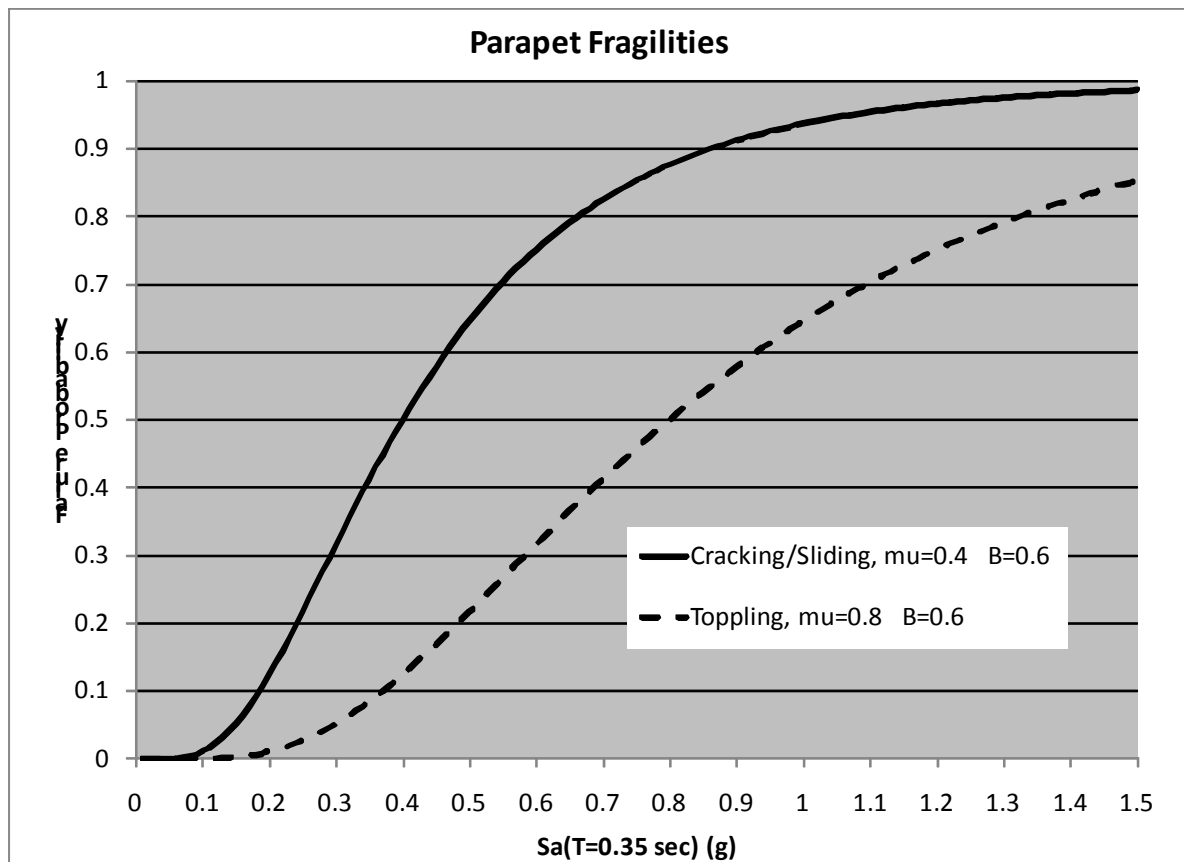


Figure 11. Proposed fragility curves for unreinforced masonry parapets with PGA as demand parameter





**Figure 12.** Proposed fragility curves for unreinforced masonry parapets with  $S_a(T=1 \text{ sec})$  as demand parameter



**Figure 13.** Proposed fragility curves for unreinforced masonry parapets with  $S_a(T=0.35 \text{ sec})$  as demand parameter

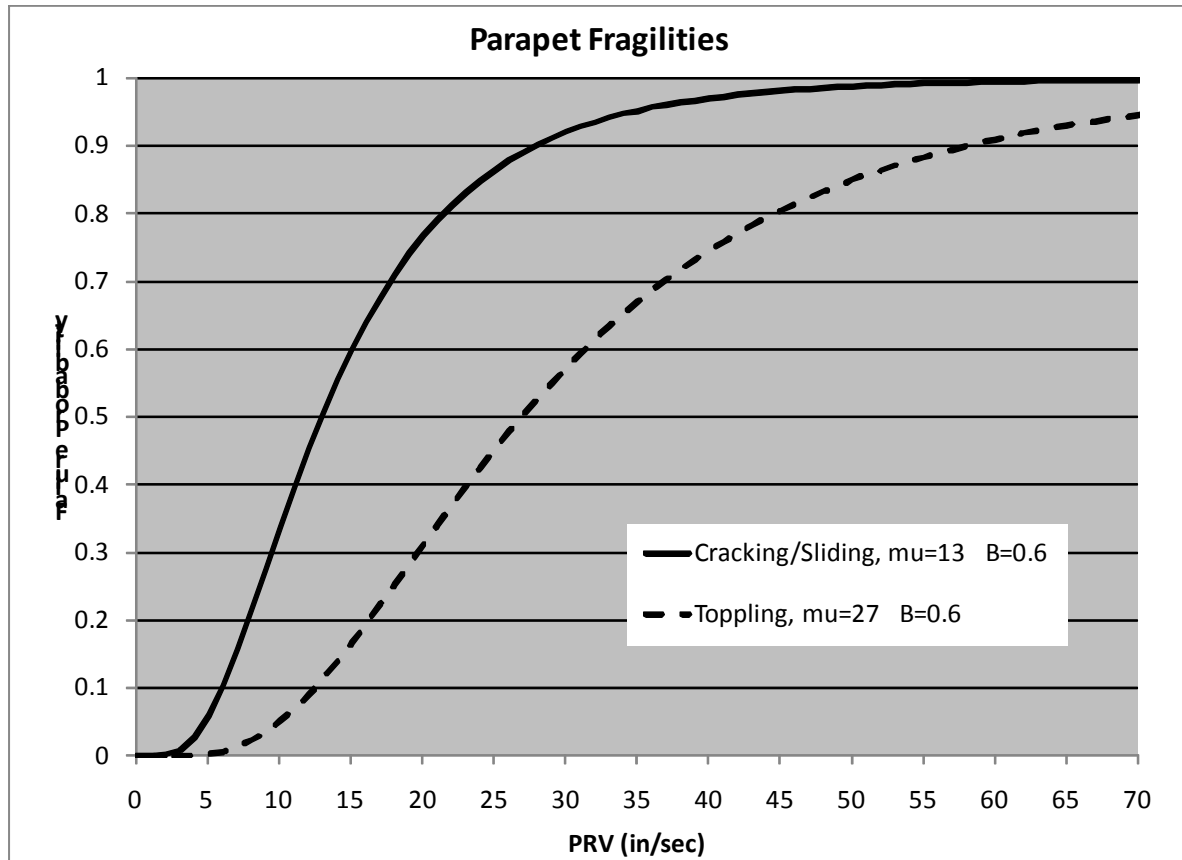


**Figure 14.** Proposed fragility curves for unreinforced masonry parapets with PRV at  $T=0.35 \text{ sec.}$  as demand parameter

## REFERENCES CITED

Aslam M, Godden WG, and Scalise DT, Earthquake Rocking Response of Rigid Bodies, Journal of the Structural Division – Proceedings of the American Society of Civil Engineers, Vol. 106, No. ST2, February 1980.

Baker and Zareian (2009) Maximum Likelihood routine for fitting log-normal curves, personal communication with H Krawinkler.

Bealle (2003). Masonry Design and Detailing for Architects and Contractors. McGraw Hill.

FEMA (2009). “Quantification of Building Seismic Performance Factors,” FEMA P-695 Report, prepared by the Applied Technology Council for the Federal Emergency Management Agency, Washington, D.C.

Housner GW, The Behavior of Inverted Pendulum Structures During Earthquakes, Bulletin of the Seismological Society of America, Vol. 53, No. 2, February 1963.

Ishiyama, Y, Motions of Rigid Bodies and Criteria for Overturning by Earthquake Excitations,

Earthquake Engineering and Structural Dynamics, Vol. 10, 635-650, 1982.

Ishiyama, Y, Criteria for Overturning of Rigid Bodies by Sinusoidal and Earthquake Excitations, Proceedings of the Eighth World Conference on Earthquake Engineering, Vol. IV – Response of Structures, July 21-28, 1984.

Lizundia, et. al, 1991. Damage to Unreinforced Masonry Buildings in the October 17, 1989 Loma Prieta Earthquake, funded by NSF and California Seismic Safety Commission, February.

Lizundia, et. al, 1997a. Development of Procedures to Enhance the Performance of Rehabilitated URM Buildings, funded by National Institute of Standards and Technology, NIST Report NIST GCR 97-724-1, August.

Lizundia, et. al, 1997b. Appendices: Development of Procedures to Enhance the Performance of Rehabilitated URM Buildings, funded by National Institute of Standards and Technology, NIST Report NIST GCR 97-724-2, August.

Meisl CS, Elwood KJ, and Ventura CE, Shake Table Tests on the Out-of-Plane Response of Unreinforced Masonry Walls, Canadian Journal of Civil Engineering, Vol. 34, 2007.

Purvance, MD, et al. Free standing block overturning fragilities: Numerical simulation and experimental validation, Earthquake Engineering and Structural Dynamics, 2008: 37:791-808

Sharif I, Meisl CS, and Elwood KJ, Assessment of ASCE 41 Height-to-Thickness Ratio Limits for URM Walls, Earthquake Spectra, Vol. 23, No. 4, November 2007.

Spanos PD, and Koh AS, Rocking of Rigid Blocks Due to Harmonic Shaking, Journal of Engineering Mechanics, Vol. 110, No. 11, November 1984.

Yim CS, Chopra AK, and Penzien J, Rocking Response of Rigid Blocks to Earthquakes, Earthquake Engineering and Structural Dynamics, Vol. 8, 1980.

#### **Revision history**

1.0	30 Nov 2010	Initial release
2.0	08 Dec 2010	Revisions to all sections - Issued to REB
3.0	28 Dec 2010	Addition of PRV, Sa(1 sec.), and Sa(0.35 sec.) as demand parameters